Environ Monit Assess (2015) 187: 382
DOI 10.1007/s10661-015-4619-y

Evaluation of three satellite-based latent heat flux algorithms over forest ecosystems using eddy covariance data

Yunjun Yao · Yuhu Zhang · Shaohua Zhao · Xianglan Li · Kun Jia

Received: 18 November 2014 / Accepted: 19 May 2015 / Published online: 28 May 2015

Abstract We have evaluated the performance of three satellite-based latent heat flux (LE) algorithms over forest ecosystems using observed data from 40 flux towers distributed across the world on all continents. These are the revised remote sensing-based Penman-Monteith LE (RRS-PM) algorithm, the modified satellite-based Priestley-Taylor LE (MS-PT) algorithm, and the semi-empirical Penman LE (UMD-SEMI) algorithm. Sensitivity analysis illustrates that both energy and vegetation terms has the highest sensitivity compared with other input variables. The validation results show that three algorithms demonstrate substantial differences in algorithm performance for estimating daily LE variations among five forest ecosystem biomes. Based on the average Nash-Sutcliffe efficiency and root-mean-squared error (RMSE), the MS-PT algorithm has high performance over both deciduous broadleaf forest (DBF) (0.81, 25.4 W/m^2) and mixed forest (MF) (0.62, 25.3 W/m^2) sites, the RRS-PM algorithm has high performance over evergreen broadleaf forest (EBF) (0.4, 28.1 W/m^2) sites, and the UMD-SEMI algorithm has high performance over both deciduous needleleaf forest (DNF) (0.78, 17.1 W/m^2) and evergreen needleleaf forest (ENF) (0.51, 28.1 W/m^2) sites. Perhaps the lower uncertainties in the required forcing data for the MS-PT algorithm, the complicated algorithm structure for the RRS-PM algorithm, and the calibrated coefficients of the UMD-SEMI algorithm based on ground-measured data may explain these differences.

Keywords Latent heat flux · Forest ecosystems · Revised remote sensing-based Penman-Monteith LE algorithm · Modified satellite-based Priestley-Taylor LE algorithm · Semi-empirical Penman LE algorithm

Y. Yao · X. Li · K. Jia
State Key Laboratory of Remote Sensing Science, School of Geography, Beijing Normal University, Beijing 100875, China

Y. Zhang (✉)
College of Resource Environment and Tourism, Capital Normal University, Beijing 100048, China
e-mail: zhang_yuhu@163.com

S. Zhao
Satellite Environment Center, Ministry of Environmental Protection, Beijing 100094, China

Introduction

Latent heat flux (LE) refers to the transferred energy during the process of evaporation of liquid water from various land surfaces (including small water bodies) and transpiration from the leaves of plants and sublimation of ice and snow (Liang et al. 2010; Vinukollu et al. 2011a; Wang and Dickinson 2012; Yao et al. 2013, 2014a, b). Especially, the amount of LE for terrestrial forest transpiration, approximately 5–30 times greater than the amount of LE for soil evaporation, has played an important role in the climate system by coupling the surface with the atmosphere, and the variable that links the water, energy, and carbon cycles (Mu et al. 2007; Fisher et al. 2008; Wang and Liang 2008; Yuan et al. 2010; Mueller et al. 2011; Yao et al.

2014c). Accurately estimating LE over forest ecosystems is therefore required to understand and simulate dynamics of surface vegetation in energy and hydrological cycles.

Numerous models with different levels of complexity and process parameterizations have been developed and widely used to for quantifying surface LE. These LE methods mainly include (1) statistical and empirical methods (Jackson et al. 1977; Wang et al. 2007; Jung et al. 2010; Mueller et al. 2011), (2) surface energy balance methods (Norman et al. 1995; Kustas and Norman 1996; Anderson et al. 1997), (3) Penman-Monteith (PM) method (Monteith 1965; Wang et al. 2010a, b; Mu et al. 2011), (4) Priestley-Taylor (PT) method (Priestley and Taylor 1972; Fisher et al. 2008; Jin et al. 2011; Yao et al. 2013), and (5) data assimilation (DA) methods (Pipunic et al. 2008; Xu et al. 2011a, b). However, most of the models described above vary in structural complexity, parameterization, and the level of data required to run them. Moreover, when applied at different surface vegetation types, these methods have resulted in large differences (Jiménez et al. 2011; Mueller et al. 2011).

In recent years, several studies have focused on estimating regional LE based on the PM and PT method driven by meteorological and remote sensing data (Cleugh et al. 2007; Fisher et al. 2008; Zhang et al. 2009, 2010; Wang et al. 2010a, b; Vinukollu et al. 2011b). Cleugh et al. (2007) proposed a simple surface resistance algorithm for the PM method using leaf area index (LAI) and other meteorological parameters. Fisher et al. (2008) designed a novel PT-based LE algorithm (PT-JPL) by introducing both atmospheric (relative humidity, RH, and vapor pressure deficit (VPD)) and eco-physiological constraints (fraction of photosynthetically active radiation, FPAR, and LAI) without using any ground-based observed data. Subsequently, Mu et al. (2011) developed a LE algorithm to generate moderate-resolution imaging spectroradiometer (MODIS) product by introducing a stomatal conductance parameterization based on environmental controlling factors and separating surface conductance over bare soil. To overcome the overestimation of canopy conductance when LAI is higher than 3, Wang et al. (2010a, b) used the normalized difference vegetation index (NDVI) and relative humidity deficit (RHD) to parameterize canopy conductance and proposed a semi-empirical Penman LE algorithm to estimate global surface LE. Although these models have proven to be effective for estimating LE at regional-scale applications, model parameters were calibrated locally, limiting the utility of the studied model to those specific locations or areas with similar meteorological and land surface conditions (Wang and Dickinson 2012; Ershadi et al. 2013).

Considering that it is difficult to select an appropriate LE algorithm for different land cover types, many scientist attempted to focus on a number of model intercomparison studies. Sumner and Jacobs (2005) compared PM and PT methods using eddy covariance (EC) observations of pasture sites in Florida and found that the PT method with a calibrated alpha coefficient outperforms the PM method. Vinukollu et al. (2011a) evaluated three LE algorithms (Surface Energy Balance System (SEBS), PM and PT algorithms) using eddy covariance observations from 16 FLUXNET tower sites and documented that PT algorithm provided the best estimates. Similarly, Chen et al. (2014) compared eight LE models, including five empirical and three process-based models, using the observed data from 23 eddy covariance towers in China and reported that the parameters of the empirical methods may have different combinations because the environmental factors of LE are not independent. Many of these intercomparison studies mainly focus on evaluation of different actual LE algorithms using few eddy covariance sites of small regions (Jiménez et al. 2011; Mueller et al. 2011; Ershadi et al. 2013). However, selection of the best LE algorithm for different forest ecosystems applications is still not documented in current method intercomparison contributions.

In this study, we evaluate the performance of three satellite-based LE algorithms, including a revised remote sensing-based Penman-Monteith LE (RRS-PM) algorithm, a modified satellite-based Priestley-Taylor LE (MS-PT) algorithm, and a semi-empirical LE (UMD-SEMI) algorithm of the University of Maryland, across a variety of forest types. Our study has two major objectives. First, we analyze the LE algorithms' structure and the sensitivity of input variables for the three satellite-based LE algorithms. Second, we evaluate the LE algorithms' performance over forest ecosystems based on 40 flux tower sites provided by FLUXNET network.

Datasets

Data at FLUXNET eddy covariance sites

Three satellite-based LE algorithms were evaluated with the flux data from six Ameriflux towers (http://public.ornl.gov/ameriflux/data-get.cfm), one Chinaflux tower (http://159.226.111.42/pingtai/LoginRe/opendata.jsp), nine Asiaflux towers (http://asiaflux.yonsei.kr/index.html) (Yu et al. 2006a, b, 2008, 2013), and 24 FLUXNET towers (http://www.fluxdata.org). These data sets include the longest continuous worldwide multisite measurements of LE, sensible heat flux (H), surface net radiation (Rn), and corresponding meteorological observations. The flux tower sites cover five major global land-surface forest biomes: deciduous broadleaf forest (DBF; 10 sites), deciduous needleleaf forest (DNF; 4 sites), evergreen broadleaf forest (EBF; 10 sites), evergreen needleleaf forest (ENF; 10 sites), and mixed forest (MF; 6 sites) (Table 1 and Fig. 1). Detailed information on site information and data gap-filling technique were available at the FLUXNET web site. The data cover the period from 2000 to 2007, and each flux tower has at least 1 year of reliable data. Although the eddy covariance method is considered best for directly measuring heat fluxes in global measurement experiments (Baldocchi et al. 2001; Gough et al. 2013), we selected the method proposed by Twine et al. (2000) to correct the LE from the FLUXNET flux towers and Chinese flux towers, due to the problem of energy imbalance.

Satellite inputs to LE algorithms

To evaluate the performance of all LE algorithms over forest ecosystems in this study for all 40 flux tower sites, the 8-day MODIS FPAR/LAI (MOD15A2) product (Myneni et al. 2002) and the 16-day MODIS NDVI/EVI (MOD13A2) product (Huete et al. 2002) with 1-km spatial resolution were used to drive three algorithms. These data were downloaded directly from the Oak Ridge National Laboratory Distributed Active Center (ORNL DAAC) web site (http://daac.ornl.gov/MODIS/). Quality control (QC) flags were examined to screen and reject poor quality LAI/FPAR and NDVI/EVI data. The daily FPAR and LAI values were temporally interpolated from the 8-day averages using linear interpolation. Similarly, the daily NDVI/EVI values were temporally interpolated from the 16-day averages using linear interpolation.

Algorithms descriptions

Revised remote sensing-based Penman-Monteith LE algorithm

Based on the beta version of the MOD16 algorithm (Mu et al. 2007), Yuan et al. (2010) developed a revised remote sensing-based PM LE (RRS-PM) algorithm by revising the equations dealing with temperature constraint for stomatal conductance and energy allocation between vegetation canopy and soil surface (Yuan et al. 2012, 2014). The RRS-PM algorithm meets Penman-Monteith equation, namely,

$$\mathrm{LE} = \frac{\Delta(R_n - G) + \rho C_p(e_s - e)/r_a}{\Delta + \gamma(1 + r_s/r_a)} \quad (1)$$

where ρ is the density of air, C_p is the specific heat of air at constant pressure, e_s is the saturated vapor pressure, e is the actual vapor pressure, Δ is the slope of the saturate vapor pressure curve, γ is the psychrometric constant, r_s and r_a are the aerodynamic and surface resistance, respectively.

In the RRS-PM algorithm, the temperature constraint (m_T) for stomatal conductance follows the equation detailed by Fisher et al.(2008) with an optimum T_{opt} set as 25 °C.

$$m_T = \exp\left(-\left(\frac{T - T_{opt}}{T_{opt}}\right)^2\right) \quad (2)$$

In the RRS-PM algorithm, the Beer-Lambert law was used to exponentially partition net radiation between the canopy (A_c) and the soil surface (A_{soil}).

$$A_{soil} = R_n \exp(-k \times \mathrm{LAI}) \quad (3)$$

$$A_c = R_n - A_{soil} \quad (4)$$

where k is extinction coefficient (0.5). The validation for 23 EC flux tower sites in China revealed higher accuracy for the RRS-PM algorithm than for the beta version of the MOD16 algorithm (Chen et al. 2014).

Table 1 A description of site conditions

Site name	Country	Land cover types	Lat	Lon	Elev	Time period	Network
NH-Bartlett Experimental Forest (US-Bar)	USA	DBF	44.06	−71.29	272	2004–2005	AmeriFlux
MA-Harvard Forest EMS Tower (HFR1) (US-Ha1)	USA	DBF	42.53	−72.17	340	2000–2006	AmeriFlux
IN-Morgan Monroe State Forest (US-MMS)	USA	DBF	39.32	−86.41	275	2000–2004	AmeriFlux
MI-Univ. of Mich. Biological Station (US-UMB)	USA	DBF	45.56	−84.71	234	2000–2003	AmeriFlux
FL-Slashpine-Austin Cary- 65 years nat regen (US-SP1)	USA	ENF	29.74	−82.22	50	2000–2005	AmeriFlux
CA-Blodgett Forest (US-Blo)	USA	ENF	38.89	−120.63	1315	2000–2006	AmeriFlux
Laoshan (LSH)	China	DNF	45.28	127.58	340	2002–2003	AsiaFlux
Southern Khentei Taiga (SKT)	Mongolia	DNF	48.35	108.65	1630	2000–2004	AsiaFlux
Tura (TUR)	Russia	DNF	64.21	100.46	250	2004–2005	AsiaFlux
Siberia Yakutsk Larch Forest Site (YLF)	Russia	DNF	62.26	129.24	220	2003–2004	AsiaFlux
Bukit Soeharto (BKS)	Indonesia	EBF	−0.86	117.04	20	2001–2002	AsiaFlux
KoFlux Gwangneung supersite (GDK)	Korea	MF	37.75	127.15	260	2004–2007	AsiaFlux
Tomakomai Flux Research Site (TMK)	Japan	MF	42.74	141.52	140	2001–2003	AsiaFlux
Teshio CC-LaG Experiment Site (TSE)	Japan	MF	45.05	142.10	70	2001–2005	AsiaFlux
Mae Klong (MKL)	Thailand	EBF	14.58	98.84	231	2003–2004	AsiaFlux
Changbaishan (CN-Cha)	China	MF	42.40	128.09	761	2003–2004	ChinaFlux
Tumbarumba (AU-Tum)	Australia	EBF	−35.66	148.15	1200	2001–2006	FLUXNET
Wallaby Creek (AU-Wac)	Australia	EBF	−37.43	145.19	545	2005–2007	FLUXNET
Santarem-Km83-Logged Forest (BR-Sa3)	Brazil	EBF	−3.02	−54.97	100	2000–2003	FLUXNET
Puechabon (FR-Pue)	France	EBF	43.74	3.59	270	2000–2006	FLUXNET
Palangkaraya (ID-Pag)	Indonesia	EBF	2.35	114.04	30	2002–2003	FLUXNET
Castelporziano (IT-Cpz)	Italy	EBF	41.71	12.38	68	2000–2006	FLUXNET
Lecceto (IT-Lec)	Italy	EBF	43.30	11.27	314	2005–2006	FLUXNET
Espirra (PT-Esp)	Portugal	EBF	38.64	−8.60	95	2002–2006	FLUXNET
UCI-1850 burn site (CA-NS1)	Canada	ENF	55.88	−98.48	260	2001–2006	FLUXNET
Quebec Boreal Cutover Site (CA-Qcu)	Canada	ENF	49.27	−74.04	392	2001–2006	FLUXNET
Bily Kriz- Beskidy Mountains (CZ-BK1)	Czech Republic	ENF	49.50	18.54	908	2000–2006	FLUXNET
Anchor Station Tharandt-Old Spruce (DE-Tha)	Germany	ENF	50.96	13.57	380	2000–2006	FLUXNET
Le Bray (after 6/28/1998) (FR-LBr)	France	ENF	44.72	−0.77	61	2000–2006	FLUXNET
Lavarone (after 3/2002) (IT-Lav)	Italy	ENF	45.96	11.28	1353	2000–2006	FLUXNET
Fyodorovskoye Wet Spruce Stand (RU-Fyo)	Russia	ENF	56.46	32.92	260	2000–2004	FLUXNET
Griffin-Aberfeldy-Scotland (UK-Gri)	UK	ENF	56.61	−3.79	340	2000–2006	FLUXNET
Brasschaat (De Inslag Forest) (BE-Bra)	Belgium	MF	51.31	4.52	16	2000–2006	FLUXNET
Vielsalm (BE-Vie)	Belgium	MF	50.31	5.99	450	2000–2006	FLUXNET
Hainich (DE-Hai)	Germany	DBF	51.79	10.45	430	2000–2006	FLUXNET
Soroe-LilleBogeskov (DK-Sor)	Denmark	DBF	55.49	11.65	40	2000–2006	FLUXNET
Fontainebleau (FR-Fon)	France	DBF	48.48	2.78	90	2005–2006	FLUXNET
Collelongo-Selva Piana (IT-Col)	Italy	DBF	41.85	13.59	1550	2000–2006	FLUXNET
Zerbolo-Parco Ticino-Canarazzo (IT-PT1)	Italy	DBF	45.20	9.06	60	2002–2004	FLUXNET
Hampshire (UK-Ham)	UK	DBF	51.15	−0.86	80	2004–2005	FLUXNET

Land cover types (*DBF* deciduous broadleaf forest, *DNF* deciduous needleleaf forest, *EBF* evergreen broadleaf forest, *ENF* evergreen needleleaf forest, *MF* mixed forest), latitude (Lat), longitude (Lon), elevation (Elev, meter), time-period, and network names are shown here

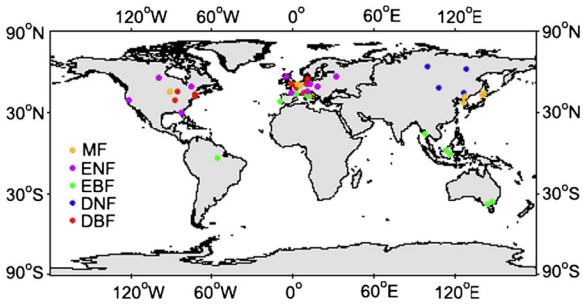

Fig. 1 Location of the 40 flux tower sites used in this study. *DBF* deciduous broadleaf forest, *DNF* deciduous needleleaf forest, *EBF* evergreen broadleaf forest, *ENF* evergreen needleleaf forest, *MF* mixed forest

Modified satellite-based Priestley-Taylor LE algorithm

The modified satellite-based Priestley-Taylor algorithm (MS-PT) is specifically designed to minimize the need for ancillary meteorological data (Vinukollu et al. 2011a; Yao et al. 2013). It only needs four variables—surface net radiation (Rn), air temperature (Ta), diurnal air temperature range (DT), and NDVI. In the MS-PT algorithm, LE is calculated by the sum of the unsaturated soil evaporation (LE_s), the canopy transpiration (LE_c), the saturated wet soil surface evaporation (LE_{ws}), and the canopy interception evaporation (LE_{ic}). The RRS-PM algorithm can be expressed as:

$$\mathrm{LE} = \mathrm{LE_s} + \mathrm{LE_c} + \mathrm{LE_{ws}} + \mathrm{LE_{ic}} \tag{5}$$

$$\mathrm{LE_s} = \alpha(1-f_{\mathrm{wet}})f_{\mathrm{sm}}\frac{\Delta}{\Delta+\gamma}(R_{\mathrm{ns}}-G) \tag{6}$$

$$\mathrm{LE_c} = \alpha(1-f_{\mathrm{wet}})f_{\mathrm{T}}f_{\mathrm{c}}\frac{\Delta}{\Delta+\gamma}R_{\mathrm{nv}} \tag{7}$$

$$LE_{ws} = \alpha f_{\mathrm{wet}}\frac{\Delta}{\Delta+\gamma}(R_{\mathrm{ns}}-G) \tag{8}$$

$$\mathrm{LE_{ic}} = \alpha f_{\mathrm{wet}}\frac{\Delta}{\Delta+\gamma}R_{\mathrm{nv}} \tag{9}$$

where α is a coefficient of the Priestley-Taylor equation (1.26), f_{wet} is the wet surface fraction, f_{sm} is the soil moisture constraint, f_{c} is the vegetation cover fraction, f_{T} is the plant temperature constraint, G is soil heat flux, R_{ns} is the surface net radiation to the soil, and R_{nv} is the surface net radiation to the vegetation.

Semi-empirical LE algorithm of the University of Maryland

To detect LE variations on a scale of several decades, Wang et al. (2010a, b) developed a semi-empirical LE (UMD-SEMI) algorithm based on the Penman equation. The UMD-SEMI algorithm considers the impacts of wind speed (WS) on LE and it can be expressed as:

$$\mathrm{ET} = a_1(\mathrm{ET_E} + \mathrm{ET_A}) + a_2(\mathrm{ET_E} + \mathrm{ET_A})^2 \tag{10}$$

$$\mathrm{ET_E} = \frac{\Delta}{\Delta+\gamma}R_{\mathrm{s}}[a_3 + a_4\mathrm{NDVI} + \mathrm{RHD}(a_5 + a_6\mathrm{NDVI})] \tag{11}$$

$$\mathrm{ET_A} = \frac{\gamma}{\Delta+\gamma}\mathrm{WS}[a_7 + \mathrm{RHD}(a_8 + a_9\mathrm{NDVI})]\mathrm{VPD} \tag{12}$$

where a_1=0.819, a_2=0.0017, a_3=0.476, a_4=0.284, a_5=−0.654, a_6=0.264, a_7=3.06, a_8=−3.86, a_9=3.64, RHD equals to 1 minus relative humidity (RH), and VPD refers to vapor pressure deficit.

Statistical analysis

We selected a simple method to analyze the sensitivity of input variables for three satellite-based LE algorithms (Wang et al. 2007; Yao et al. 2012), and this formula can be written as:

$$\mathrm{SRC} = \frac{\partial \mathrm{LE}}{\partial V(x)} \tag{13}$$

where SRC is the sensitivity coefficient, $V(x)$ is the input variable (e.g., Rn, Ta, NDVI). We have also summarized the coefficient of determination (R^2), the root-mean-squared error (RMSE), the Nash-Sutcliffe efficiency coefficient (NSE), and the average bias and p values for the estimated LE and those derived from tower data to evaluate the relative predictive errors for three LE algorithms. The Nash-Sutcliffe efficiency represents a normalized statistic that determines the relative magnitude of the residual variance (noise)

compared to the measured data variance (Nash and Sutcliffe 1970) and is expressed as:

$$\mathrm{NSE} = 1 - \frac{\sum_{i=1}^{n} \left(\mathrm{LE}_i^{\mathrm{obs}} - \mathrm{LE}_i^{\mathrm{sim}}\right)^2}{\sum_{i=1}^{n} \left(\mathrm{LE}_i^{\mathrm{obs}} - \mathrm{LE}_{\mathrm{mean}}\right)^2} \quad (14)$$

where $\mathrm{LE}_i^{\mathrm{obs}}$ is the ith observed LE, $\mathrm{LE}_i^{\mathrm{sim}}$ is the ith simulated LE, $\mathrm{LE}_{\mathrm{mean}}$ is the mean of the observed LE, and n is the total number of observations. NSE varies from $-\infty$ to 1.0, with a NSE=1 being the optimal value (Moriasi et al. 2007; Ershadi et al. 2013).

Results

Sensitivity analysis of three satellite-based LE algorithms

Given the great difference in three satellite-based LE algorithm structures and the input variables, it is of interest to examine the sensitivity of input variables for three satellite-based LE algorithms. Rn, Ta, LAI, and RH are the input variables for the RRS-PM algorithm. As illustrated for the MS-PT algorithm, except for Rn and Ta, it also acquires NDVI and DT. The UMD-SEMI algorithm is the only method that explicitly includes wind speed, which may play an important role in annual or decadal LE (Wang et al. 2010a, b; McVicar et al. 2012). The energy term of the UMD-SEMI algorithm is Rs rather than Rn. The averaged LE varies at all flux towers up to ±20 % for the MS-PT and RRS-PM algorithms by changing Rn with ±20 and ±16 %, respectively (Fig. 2). For the UMD-SEMI algorithm, in response to the ±20 % change in LE, Rs varies by ±18 %. LE varies by ±20 % for the RRS-PM and UMD-SEMI algorithms by changing RH with ±4 and ±6 %, respectively. However, for the MS-PT algorithm, LE relatively increases up to 3 % for DT change of −20 %. In response to the change in NDVI (LAI) with ±20 % for both MS-PT and UMD-SEMI (RRS-PM) algorithms, LE varies by ±10 and ±8 % (±6 %) at all flux towers. LE estimated by the UMD-SEMI algorithm varies by ±4 % for WS change of ±20 %. Overall, LE estimation by three algorithms shows different sensitivity orders: Rn>LAI>RH>Ta for the RRS-PM algorithm, Rn>NDVI>Ta>DT for the MS-PT algorithm, and Rs>NDVI>RH>Ta>WS for the UMD-SEMI algorithm.

For the above three LE algorithms, energy (Rn or Rs) and vegetation (NDVI or LAI) terms account for more than 78 % variation of LE. The contribution of the energy term (Rn or Rs) is the highest in the three LE algorithms because these algorithms are calculated as the sum of the surface energy balance term. Hwang and Choi (2013) found the sensitivity orders: Rn>LAI>Pa for the revised remote sensing-based PM model. Yao et al. (2014b) considered the sensitivity orders of estimated LE using the MS-PT algorithm with Rn (±20 % change of LE for ±20 % change of the variable)>NDVI (±10 %)>Ta and DT (less than ±7 %) at different land cover types. Besides Rn, the dependency of NDVI (or LAI) in these algorithms is higher in all flux towers as vegetation amount quantified by vegetation index (NDVI) and LAI affect the vegetation photosynthesis and transpiration (Tucker 1979; Wang and Liang 2008; Yao et al. 2013, 2014a). Canopy conductance, which is directly related with plant transpiration, and vegetation index (or LAI) represented a nonlinear relationship. Wang and Dickinson (2012) pointed out that many equations will overestimate canopy conductance when LAI is higher than 3 or 4, and using vegetation index can effectively correct this issue. Compared with energy and vegetation terms, other variables play a minor role.

Comparisons of three satellite-based LE algorithms over forest ecosystems

Three satellite-based LE algorithms demonstrate substantial differences in algorithm performance for estimating daily LE variations among five forest ecosystem types (Fig. 3). For both ENF and EBF, all algorithms demonstrate low performance with high RMSE and low R^2. In contrast, all algorithms exhibit good performance over DBF and DNF sites. This may be attributed to the fact that strong seasonality for vegetation indices or LAI effectively characterizes the variations in the LE of broadleaf forest while reliable vegetation information is difficult to acquire for evergreen forest because seasonal evergreen forest variation is less evident (Yebra et al. 2013). For all five forest types, the MS-PT algorithm has a good overall performance and exhibits the highest R^2 and RRS-PM shows the lowest R^2 because the MS-PT algorithm has partitioned total evaporation (canopy transpiration, soil evaporation, wet canopy evaporation) and its lower uncertainties in the required

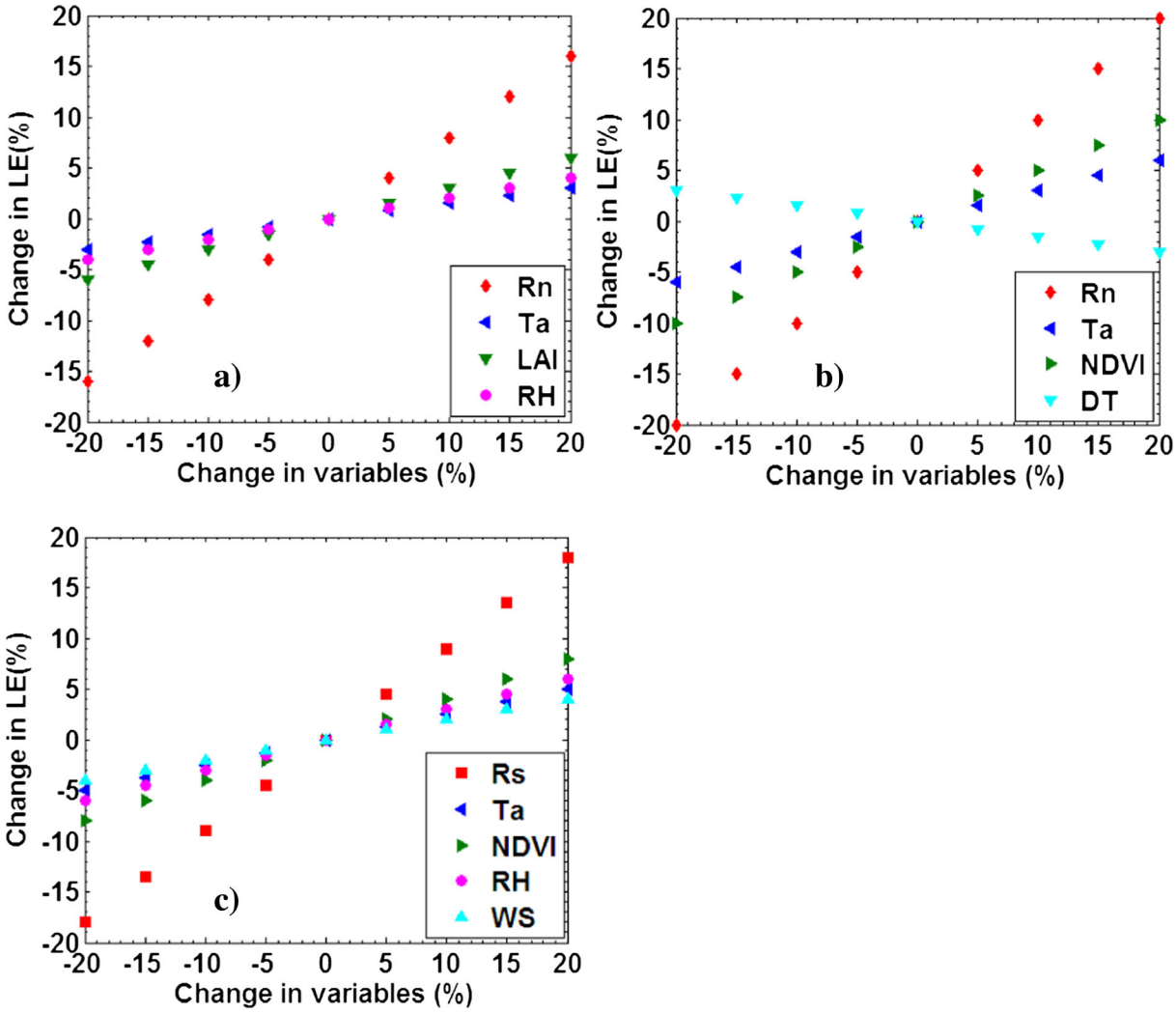

Fig. 2 Sensitivity analysis of the LE estimated by the **a** RRS-PM, **b** MS-PT, and **c** UMD-SEMI algorithms with the corresponding input variables, respectively

forcing data. The second good model is the UMD algorithm and the performance of the RRS-PM algorithm is ranked third.

For a given forest type, algorithm performance differs greatly (Figs. 3 and 4). For all DBF sites, the MS-PT algorithm shows the highest performance with higher R^2 (averaged R^2=0.79) and NSE (averaged NSE=0.81), and lower RMSE (averaged RMSE=25.4 W/m^2) when compared with the other two algorithms while the RRS-PM algorithm shows the lowest performance. For all DNF sites, the RRS-PM algorithm has the highest average RMSE (20.3 W/m^2), and the UMD-SEMI algorithm has the lowest RMSE (17.1 W/m^2) and the greatest average NSE (0.78). It is clear that the MS-PT and UMD-SEMI algorithms both overestimate terrestrial LE, but the RRS-PM algorithm underestimates terrestrial LE for all DNF sites. For all EBF sites, the RRS-PM algorithm has the lowest average RMSE (28.1 W/m^2), with average R^2 of 0.55 and average NSE of 0.4 for all EBF sites. However, the MS-PT algorithm has the highest R^2 despite of its higher RMSE. For all ENF sites, the UMD-SEMI algorithm has the lowest average RMSE (28.1 W/m^2), with average bias of 5.7 W/m^2 and with average NSE of 0.51. Considering the UMD-SEMI algorithm was calibrated using the data from 64 flux tower sites provided by FLUXNET projects, the performance of the UMD-SEMI algorithm is strongly related to the regression coefficients (Yao et al. 2013, 2014a). For all MF sites, the performance of the MS-PT algorithm with the highest average NSE (0.62) and the

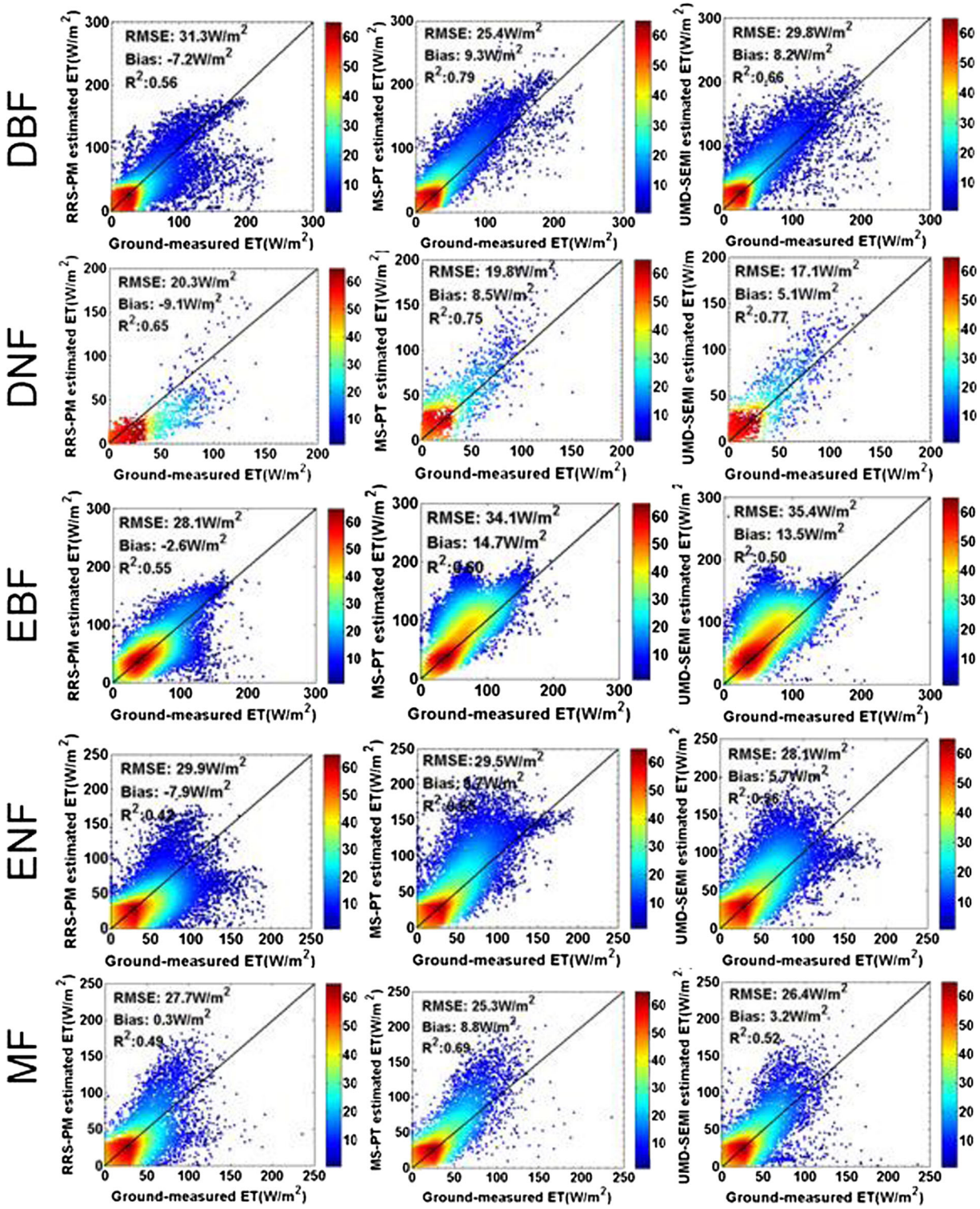

Fig. 3 Observed LE at eddy covariance sites versus estimated LE from three algorithms

lowest average RMSE (25.3 W/m^2) is higher than both the RRS-PM and UMD-SEMI algorithms. In general, MF has the higher canopy conductance than that of deciduous forests (Eugster et al. 2000) and perhaps the

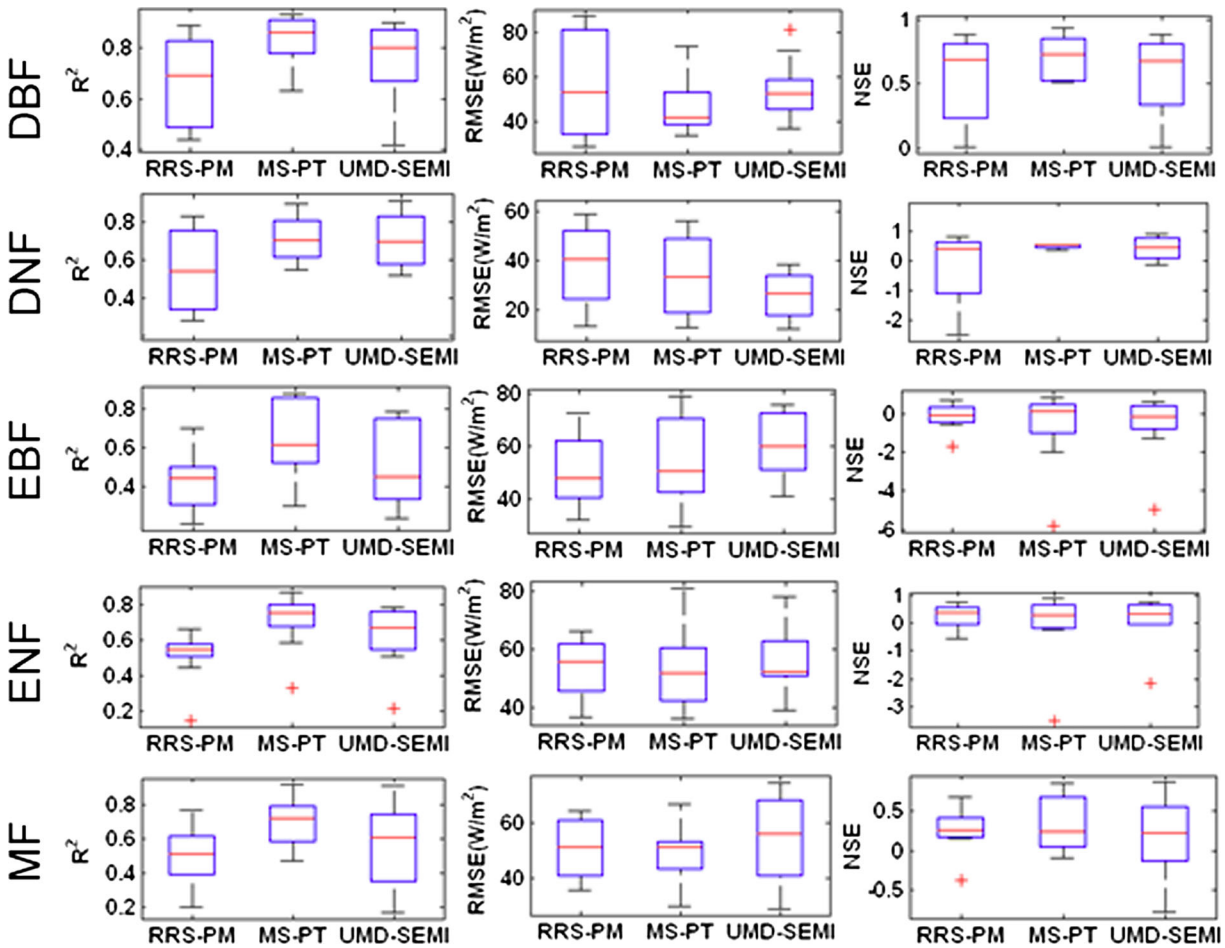

Fig. 4 Model performance of three LE algorithms for estimating daily LE for five forest biomes

MS-PT algorithm may capture this information by parameterization of the vegetation index.

Figure 5 shows an example of the seasonal cycles of the 8-day LE average simulated by three satellite-based latent heat flux algorithms at different type sites. Distinct seasonal cycles of LE can be found at different sites. In general, the measured and predicted seasonal curves are in good agreement. For DBF, DNF, ENF, and MF sites, the estimated LE is higher in summer when the Rs, Ta, and vegetation index are maximal. During spring and fall, the estimated LE is smaller due to the decreasing Rs and Ta. In contrast, compared with other forests, the LE for the EBF site is high in winter. Although the LE estimated by the three satellite-based algorithms has similar seasonal variation, in comparison to the RRS-PM and UMD-SEMI algorithms, the MS-PT algorithm yields seasonal LE variations that are closest to the ground-measured values at most forest types and this is generally consistent with the previous literature (Yao et al. 2014a, b; Ershadi et al. 2013; Chen et al. 2014). Ershadi et al. (2013) used FLUXNET data to evaluate four LE algorithms (SEBS, PM, PT, and complementary method) and found that the PT method has improved performance compared to the PM method. Chen et al. (2014) compared eight LE models, including five empirical and three process-based models and reported that although the three process-based models showed high model performance across the validation sites, there were substantial differences among them in the temporal and spatial patterns of LE.

Discussion

Regulators of the three LE algorithms

Available energy, moisture demand, and atmospheric evaporative demand have been considered as the three

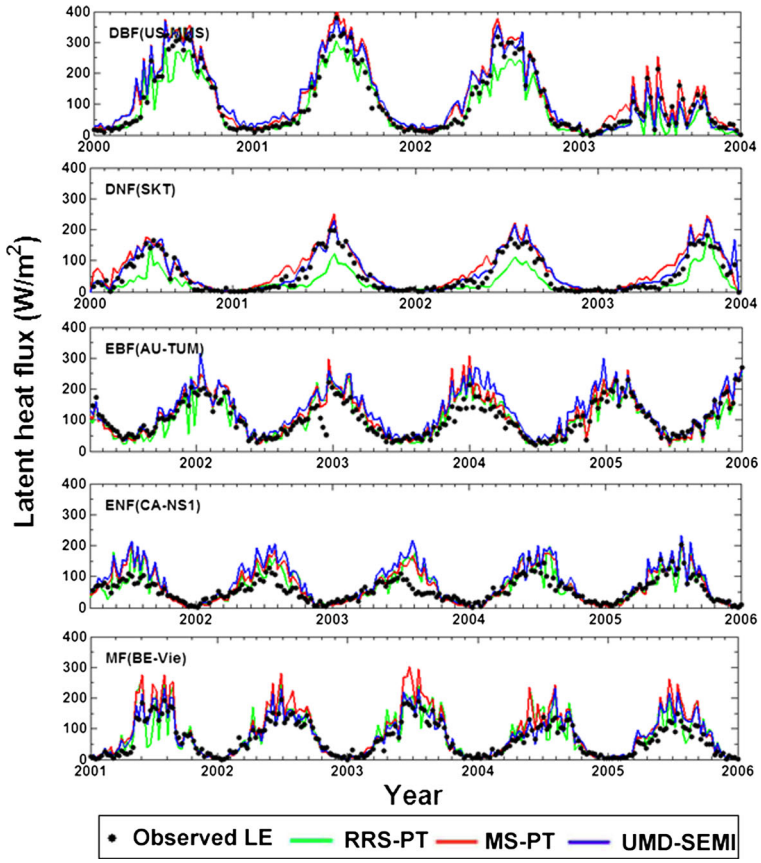

Fig. 5 Example of a time series for the 8-day LE average as measured and estimated using three algorithms for five forest biomes

most factors controlling LE. In this study, the three LE algorithms have strongly correlated with Rn (Rs) because it has been widely recognized as the most important parameter that varies with spatiotemporal variation in LE in terrestrial ecosystems (Wang and Dickinson 2012). However, Rn (Rs) exerts greater influence on energy-limited water-yielding catchments than water-limited (Nemani et al. 2003; McVicar et al. 2012; Wang and Dickinson 2012). McVicar et al. (2012) mapped the global distribution of areas where LE was energy-limited or water-limited to conclude that energy drives LE in both tropical ecosystems (mainly EBF) and high-latitude ecosystems (mainly ENF), and water drives LE in arid regions. Therefore, most EBF trees of tropical regions sustain elevated LE during the dry season through deep roots and most ENF trees in high-latitude regions are less water stressed because of their slow transpiration (Karam and Bras 2008; Wang and Dickinson 2012).

Moisture demand is another key factor in determining LE in most ecosystems, especially in semiarid and arid regions. Satellite-derived NDVI and LAI are good at characterizing the spatial variability of soil and vegetation moisture. Therefore, many scientists attempted to use NDVI or LAI as a surrogate for vegetation moisture and use RH to replace soil moisture to develop satellite-based LE algorithms (Fisher et al. 2008; Mu et al. 2011; Yuan et al. 2010; Wang et al. 2010a, b). The three algorithms in this study have improved the accuracy of LE simulation by integrating satellite-based vegetation parameters (NDVI or LAI).

WS, as an aerodynamic controlling variable of atmospheric evaporative demand during the evapotranspiration (ET) process, also contributes to the long-term variation in LE (Wang et al. 2010a, b; McVicar et al. 2012). Several studies have focused on the causes of evaporative dynamics without considering WS, whereas the UMD-SEMI algorithm clearly illustrates the contributions of WS to LE (Mu et al. 2007; Fisher et al. 2008; Yao et al. 2013). Although many LE algorithms without WS have higher accuracy compared with the UMD-SEMI algorithm, detection of long-term variation in terrestrial LE may cause large uncertainty when ignoring the impacts of WS on LE.

Performance of the three LE algorithms

Although the three satellite-based LE algorithms performed well in most forest sites and displayed seasonality in its performance over the majority of the flux towers, the results of this study illustrated some limitations in the application of the three algorithms. We found that the RRS-PM algorithm underestimated LE for most deciduous forests flux tower sites and in winter, the performance of the RRS-PM algorithm is low because of large errors resulting in LE underestimation. In theory, the RRS-PM algorithm should outperform the MS-PT model because its theoretical advances of the PM approach over the PT method (Ershadi et al. 2013). However, surface resistance parameterization technique is complicated and the uncertainties in forcing data reduced the accuracy of RRS-PM-based LE estimation (Mu et al. 2007; Yuan et al. 2010; Chen et al. 2014; Ershadi et al. 2013). Yuan et al. (2010) found that choice of vegetation and temperature parameterization will lead to great impact on RRS-PM-based LE estimation. Ershadi et al. (2013) also reported that the surface resistance parameterization is more important than the actual structure of the algorithm, which affected the RRS-PM algorithm.

Compared with the RRS-PM algorithm, the MS-PT algorithm demonstrated the most consistent performance for most forests sites because this algorithm does not require aerodynamic and surface resistances to reduce the uncertainties in forcing data. However, the MS-PT algorithm reduced performance for the ENF tower sites and this may be resulted from the limitation of NDVI in capturing the vegetation seasonal variation of this type (Xiao et al. 2004; Ershadi et al. 2013). In addition, Rn and Ta are the main driving factors for the MS-PT algorithm and they generally have lower uncertainty in observations (Yao et al. 2013; Ershadi et al. 2013). Similar issues in the performance of the PT algorithm have been documented in substantial previous studies (Fisher et al. 2008; Vinukollu et al. 2011a; Yao et al. 2014b). Vinukollu et al. (2011a) reported the good performance of the PT algorithm in 12 eddy covariance tower sites. Yao et al. (2014b) found that compared with the PT-JPL algorithm, the MS-PT algorithm improves the LE estimates at 40 eddy covariance flux tower sites.

The UMD-SEMI algorithm performed well in ENF sites, which may be attributed to the coefficients calibration using ground-measured data from most ENF sites. Although the UMD-SEMI algorithm ignores explicit biophysical mechanisms, it provides a simple yet seemingly robust method by building functional relationships between the LE and predictor variables (Wang et al. 2010a, b). A similar conclusion has been reported by Wang et al. (2010a, b); the 16-day average daily LE can be reasonably predicted with an average correlation coefficient of 0.94 and average RMSE of 17 W/m^2 using 64 FLUXNET sites. However, the representativeness of the limited training dataset will lead to large uncertainties by extrapolating other regions (Jung et al. 2010; Wang and Dickinson 2012; Chen et al. 2014). Chen et al. (2014) found that the parameters of the UMD-SEMI algorithm may have different combination because the environmental factors of ET are not independent.

The possible sources of uncertainty in the three satellite-based LE algorithms may stem from: (1) the errors of the ground-measured variables (Hollinger and Richardson 2005; Richardson et al. 2006; Jenkins et al. 2007), (2) the biases of the satellite-derived LAI retrieval, (3) the energy imbalance issue of the eddy covariance method, (4) the spatial scale mismatch between flux tower site and satellite-derived NDVI and LAI, and (5) the uncertainties inherent in the structure of the three algorithms for coefficients parameterization. The three algorithm used in this study are all developed with high-quality tower scale dataset. Therefore, application of these algorithms at large spatial scale will lead to large uncertainties.

Conclusion

The goal of the study was to evaluate three satellite-based LE algorithms over forest ecosystems using ground-measured data collected from 40 eddy covariance flux tower sites provided by the FLUXNET project. The LE algorithms used in this study include the RRS-PM algorithm, the MS-PT algorithm, and the UMD-SEMI algorithm. Given the great difference in the three satellite-based LE algorithm structures and the input variables, we first analyzed the sensitivity of input variables for the three satellite-based LE algorithms. Furthermore, we compared the three LE algorithms' performance over forest ecosystems.

Results of the sensitivity analysis of input variables for the three satellite-based LE algorithms illustrate that overall, LE estimation by the three algorithms shows

different sensitivity orders: Rn>LAI>RH>Ta for the RRS-PM algorithm, Rn>NDVI>Ta>DT for the MS-PT algorithm, and Rs>NDVI>RH>Ta>WS for the UMD-SEMI algorithm. For the three LE algorithms, energy (Rn or Rs) and vegetation (NDVI or LAI) terms can account for more than 78 % variation of LE. Results of the evaluation and intercomparison among these algorithms show that the three satellite-based LE algorithms demonstrate substantial differences in algorithm performance for estimating daily LE variations among five forest biomes. The MS-PT algorithm has the high performance over both DBF and MF sites, the RRS-PM algorithm has the lowest average RMSE (28.1 W/m^2) over EBF sites, and the UMD-SEMI algorithm has the high average NSE of 0.51 over ENF sites and average NSE of 0.78 over DNF sites. Regulators and uncertainties of the three LE algorithms are also discussed.

Acknowledgments The authors thank Dr. Liang Sun, Dr. Xianhong Xie, Dr. Jie Cheng, Dr. Xiaotong Zhang, Dr. Bo Jiang, and Dr. Xiang Zhao from Beijing Normal University, China, for their suggestions. This work used eddy covariance data acquired by the FLUXNET community and in particular by the following networks: AmeriFlux (US Department of Energy, Biological and Environmental Research, Terrestrial Carbon Program (DE-FG02-04ER63917 and DE-FG02-04ER63911)), AfriFlux, AsiaFlux, CarboAfrica, CarboEuropeIP, CarboItaly, CarboMont, ChinaFlux, Fluxnet-Canada (supported by CFCAS, NSERC, BIOCAP, Environment Canada, and NRCan), GreenGrass, KoFlux, LBA, NECC, OzFlux, TCOS-Siberia, USCCC. We acknowledge the financial support to the eddy covariance data harmonization provided by the CarboEuropeIP, FAO-GTOS-TCO, iLEAPS, Max Planck Institute for Biogeochemistry, National Science Foundation, University of Tuscia, Université Laval, Environment Canada, and US Department of Energy and the database development and technical support from the Berkeley Water Center, Lawrence Berkeley National Laboratory, Microsoft Research eScience, Oak Ridge National Laboratory, University of California, Berkeley, and the University of Virginia. This work was also partially supported by the National Science and Technology Support Plan During the 12th Five-year Plan Period of China (No.2012BAC19B03 and 2013BAC10B01), the Natural Science Fund of China (41201331 and 41301353), and the Fundamental Research Funds for the Central Universities (2013YB34 and 2013YB42).

References

Anderson, M., Norman, J., Diak, G., Kustas, W., & Mecikalski, J. (1997). A two-source time-integrated model for estimating surface fluxes using thermal infrared remote sensing. *Remote Sensing of Environment, 60*, 195–216.

Baldocchi, D., Falge, E., Gu, L., Olson, R., Hollinger, D., Running, S., Anthoni, P., Bernhofer, C., Davis, K., Evans, R., Fuentes, J., Goldstein, A., Katul, G., Law, B., Lee, X., Malhi, Y., Meyers, T., Munger, W., Oechel, W., Paw, K., Pilegaard, K., Schmid, H., Valentini, R., Verma, S., Vesala, T., Wilson, K., & Wofsy, S. (2001). FLUXNET: a new tool to study the temporal and spatial variability of ecosystem-scale carbon dioxide, water vapor and energy flux densities. *Bulletin of the American Meteorological Society, 82*, 2415–2434.

Chen, Y., Xia, J., Liang, S., Feng, J., Fisher, J., Li, X., Li, X., Liu, S., Ma, Z., Miyata, A., Mu, Q., Sun, L., Tang, J., Wang, K., Wen, J., Xue, Y., Yu, G., Zha, T., Zhang, L., Zhang, Q., Zhao, T., Zhao, L., & Yuan, W. (2014). Comparison of satellite-based evapotranspiration models over terrestrial ecosystems in China. *Remote Sensing of Environment, 140*, 279–293.

Cleugh, H., Leuning, R., Mu, Q., & Running, S. (2007). Regional evaporation estimates from flux tower and MODIS satellite data. *Remote Sensing of Environment, 106*, 285–304.

Ershadi, A., McCabe, M., Evans, J., Chaney, N., & Wood, E. (2013). Multi-site evaluation of terrestrial evaporation models using FLUXNET data. *Agricultural and Forest Meteorology, 187*, 46–61.

Eugster, W., Rouse, W., Pielke, R., Sr., Mcfadden, J., Baldocchi, D., Kittel, T. F., Stuart Chapin, F., III, Liston, G., Vidale, P., Vaganov, E., & Chambers, S. (2000). Land-atmosphere energy exchange in Arctic tundra and boreal forest: available data and feedbacks to climate. *Global Change Biology, 6*, 84–115.

Fisher, J., Tu, K., & Baldocchi, D. (2008). Global estimates of the land atmosphere water flux based on monthly AVHRR and ISLSCP-II data, validated at 16 FLUXNET sites. *Remote Sensing of Environment, 112*, 901–919.

Gough, C., Hardiman, B., Nave, L., et al. (2013). Sustained carbon uptake and storage following moderate disturbance in a Great Lakes forest. *Ecological Applications, 23*, 1202–1215.

Hollinger, D. Y., & Richardson, A. D. (2005). Uncertainty in eddy covariance measurements and its application to physiological models. *Tree Physiology, 25*, 873–885.

Huete, A., Didan, K., Miura, T., Rodriguez, E., Gao, X., & Ferreira, L. (2002). Overview of the radiometric and biophysical performance of the MODIS vegetation indices. *Remote Sensing of Environment, 83*, 195–213.

Hwang, K., & Choi, M. (2013). Seasonal trends of satellite-based evapotranspiration algorithms over a complex ecosystem in East Asia. *Remote Sensing of Environment, 137*, 244–263.

Jackson, R., Reginato, R., & Idso, S. (1977). Wheat canopy temperature: a practical tool for evaluating water requirements. *Water Resources Research, 13*, 651–656.

Jenkins, J., Richardson, A., Braswell, B., Ollinger, S., Hollinger, D., & Smith, M. (2007). Refining light-use efficiency calculations for a deciduous forest canopy using simultaneous tower-based carbon flux and radiometric measurements. *Agricultural and Forest Meteorology, 143*, 64–79.

Jiménez, C., Prigent, C., Mueller, B., Seneviratne, S., McCabe, M., Wood, E., Rossow, W., Balsamo, G., Betts, A., Dirmeyer, P., Fisher, J., Jung, M., Kanamitsu, M., Reichle, R., Reichstein, M., Rodell, M., Sheffield, J., Tu, K., & Wang, K. (2011). Global intercomparison of 12 land surface heat flux estimates. *Journal of Geophysical Research, 116*, D02102.

Jin, Y., Randerson, J., & Goulden, M. (2011). Continental-scale net radiation and evapotranspiration estimated using MODIS satellite observations. *Remote Sensing of Environment, 115*, 2302–2319.

Jung, M., Reichstein, M., Ciais, P., Seneviratne, S., Sheffield, J., Goulden, M., Bonan, G., Cescatti, A., Chen, J., Richard, D., Dolman, A., Eugster, W., Gerten, D., Gianelle, D., Gobron, N., Heinke, J., Kimball, J., Law, B., Montagnani, L., Mu, Q., Mueller, B., Oleson, K., Papale, D., Richardson, A., Roupsard, O., Running, S., Tomelleri, E., Viovy, N., Weber, U., Williams, C., Wood, E., Zaehle, S., & Zhang, K. (2010). Recent decline in the global land evapotranspiration trend due to limited moisture supply. *Nature, 467*, 951–954.

Karam, H., & Bras, R. (2008). Climatological basin-scale Amazonian evapotranspiration estimated through a water budget analysis. *Journal of Hydrometeorology, 9*, 1048–1060.

Kustas, W., & Norman, J. (1996). Use of remote sensing for evapotranspiration monitoring over land surfaces. *Hydrological Sciences Journal, 41*, 495–516.

Liang, S., Wang, K., Zhang, X., & Wild, M. (2010). Review on estimation of land surface radiation and energy budgets from ground measurements, remote sensing and model simulations. *IEEE Journal of Selected Topics in Applied Earth Observations and Remote Sensing, 3*, 225–240.

McVicar, T., Roderick, M., Donohue, R., Li, L., Van Niel, T., Thomas, A., Grieser, J., Jhajharia, D., Himri, Y., Mahowald, N., Mescherskaya, A., Kruger, A., Rehman, S., & Dinpashoh, Y. (2012). Global review and synthesis of trends in observed terrestrial near-surface wind speeds: implications for evaporation. *Journal of Hydrology, 416–417*, 182–205.

Monteith, J. (1965). Evaporation and environment. *Symposia of the Society for Experimental Biology, 19*, 205–224.

Moriasi D, Arnold J, Van Liew M, Bingner R, Harmel R, Veith T (2007) Model evaluation guidelines for systematic quantification of accuracy in watershed simulations. American Society of Agricultural Engineers, St. Joseph, MI, 16, ETATS-UNIS.

Mu, Q., Heinsch, F., Zhao, M., & Running, S. (2007). Development of a global evapotranspiration algorithm based on MODIS and global meteorology data. *Remote Sensing of Environment, 111*, 519–536.

Mu, Q., Zhao, M., & Running, S. (2011). Improvements to a MODIS global terrestrial evapotrans piration algorithm. *Remote Sensing of Environment, 115*, 1781–1800.

Mueller, B., Seneviratne, S., Jiménez, C., Corti, T., Hirschi, M., Balsamo, G., Ciais, P., Dirmeyer, P., Fisher, J., Guo, Z., Jung, M., Maignan, F., McCabe, M., Reichle, R., Reichstein, M., Rodell, M., Sheffield, J., Teuling, A., Wang, K., Wood, E., & Zhang, Y. (2011). Evaluation of global observations-based evapotranspiration datasets and IPCC AR4 simulations. *Geophysical Research Letters, 38*, L06402.

Myneni, R., Hoffman, S., Knyazikhin, Y., Privette, J., Glassy, J., Tian, J., Wang, Y., Song, X., Zhang, Y., Smith, G., Lotsch, A., Friedl, M., Morisette, J., Votava, P., Nemani, R., & Running, S. (2002). Global products of vegetation leaf area and fraction absorbed PAR from year one of MODIS data. *Remote Sensing of Environment, 83*, 214–231.

Nash, J., & Sutcliffe, J. (1970). River flow forecasting through conceptual models part I: a discussion of principles. *Journal of Hydrology, 10*, 282–290.

Nemani, R., Keeling, C., Hashimoto, H., Jolly, W., Piper, S., Tucker, C., Myneni, R., & Running, S. (2003). Climate-driven increases in global terrestrial net primary production from 1982 to 1999. *Science, 300*, 1560–1563.

Norman, J., Kustas, W., & Humes, K. (1995). A two-source approach for estimating soil and vegetation energy fluxes in observations of directional radiometric surface temperature. *Agricultural and Forest Meteorology, 77*, 263–293.

Pipunic, R., Walker, J., & Western, A. (2008). Assimilation of remotely sensed data for improved latent and sensible heat flux prediction: a comparative synthetic study. *Remote Sensing of Environment, 112*, 1295–1305.

Priestley, C., & Taylor, R. (1972). On the assessment of surface heat flux and evaporation using large-scale parameters. *Monthly Weather Review, 100*, 81–92.

Richardson, A. D., Hollinger, D. Y., Davis, K. J., Flanagan, L. B., Katul, G. G., Stoy, P. C., Verma, S. B., & Wofsy, S. C. (2006). A multi-site analysis of uncertainty in tower-based measurements of carbon and energy fluxes. *Agricultural and Forest Meteorology, 136*, 1–18.

Sumner, D., & Jacobs, J. (2005). Utility of Penman-Monteith Priestley-Taylor reference evapotranspiration, and pan evaporation methods to estimate pasture evapotranspiration. *Journal of Hydrology, 308*, 81–104.

Tucker, C. (1979). Red and photographic infrared linear combinations for monitoring. *Remote Sensing of Environment, 8*, 127–150.

Twine, T., Kustas, W., Norman, J., Cook, D., Houser, P., Meyers, T., Prueger, J., Starks, P., & Wesely, M. (2000). Correcting eddy-covariance flux underestimates over a grassland. *Agricultural and Forest Meteorology, 103*, 279–300.

Vinukollu, R., Wood, E., Ferguson, C., & Fisher, J. (2011a). Global estimates of evapotranspiration for climate studies using multisensory remote sensing data: evaluation of three process-based approaches. *Remote Sensing of Environment, 115*, 801–823.

Vinukollu, R., Meynadier, R., Sheffield, J., & Wood, E. (2011b). Multi-model, multi-sensor estimates of global evapotranspiration: climatology, uncertainties and trends. *Hydrological Processes, 25*, 3993–4010.

Wang, K., & Dickinson, R. (2012). A review of global terrestrial evapotranspiration: observation, modeling, climatology, and climatic variability. *Reviews of Geophysics, 50*, RG2005.

Wang, K., & Liang, S. (2008). An improved method for estimating global evapotranspiration based on satellite determination of surface net radiation, vegetation index, temperature, and soil moisture. *Journal of Hydrometeorology, 9*, 712–727.

Wang, K., Wang, P., Li, Z., Cribb, M., & Sparrow, M. (2007). A simple method to estimate actual evapotranspiration from a combination of net radiation, vegetation index, and temperature. *Journal of Geophysical Research, 112*, D15107.

Wang, K., Dickinson, R., Wild, M., Liang, S., Wang, K., Dickinson, R., Wild, M., & Liang, S. (2010a). Evidence for decadal variation in global terrestrial evapotranspiration between 1982 and 2002. Part 1: model development. *Journal of Geophysical Research, 115*, D20112.

Wang, K., Dickinson, R., Wild, M., & Liang, S. (2010b). Evidence for decadal variation in global terrestrial evapotranspiration between 1982 and 2002. Part 2: results. *Journal of Geophysical Research, 115*, D20113.

Xiao, X., Hollinger, D., Aber, J., Goltz, M., Davidson, E., Zhang, Q., & Moore Iii, B. (2004). Satellite-based modeling of gross primary production in an evergreen needleleaf forest. *Remote Sensing of Environment, 89*, 519–534.

Xu, T., Liang, S., & Liu, S. (2011a). Estimating turbulent fluxes through assimilation of geostationary operational environmental satellites data using ensemble Kalman filter. *Journal of Geophysical Research, 116*, D09109.

Xu, T., Liu, S., Liang, S., & Qin, J. (2011b). Improving predictions of water and heat fluxes by assimilating MODIS land surface temperature products into common land model. *Journal of Hydrometeorology, 12*, 227–244.

Yao, Y., Liang, S., Qin, Q., Wang, K., Liu, S., & Zhao, S. (2012). Satellite detection of increases in global land surface evapotranspiration during 1984-2007. *International Journal of Digital Earth, 5*, 299–318.

Yao, Y., Liang, S., Cheng, J., Liu, S., Fisher, J., Zhang, X., Jia, K., Zhao, X., Qin, Q., Zhao, B., Han, S., Zhou, G., Zhou, G., Li, Y., & Zhao, S. (2013). MODIS-driven estimation of terrestrial latent heat flux in China based on a modified Priestly-Taylor algorithm. *Agricultural and Forest Meteorology, 171–172*, 187–202.

Yao, Y., Liang, S., Li, X., Hong, Y., Fisher, J., Zhang, N., Chen, J., Cheng, J., Zhao, S., Zhang, X., Jiang, B., Sun, L., Jia, K., Wang, K., Chen, Y., Mu, Q., & Feng, F. (2014a). Bayesian multimodel estimation of global terrestrial latent heat flux from eddy covariance, meteorological, and satellite observations. *Journal of Geophysical Research, 119*, 4521–4545.

Yao, Y., Liang, S., Zhao, S., Zhang, Y., Qin, Q., Cheng, J., Jia, K., Xie, X., Zhang, N., & Liu, M. (2014b). Validation and application of the modified satellite-based Priestley-Taylor algorithm for mapping terrestrial evapotranspiration. *Remote Sensing, 6*, 880–904.

Yao, Y., Liang, S., Xie, X., Cheng, J., Jia, K., Li, Y., & Liu, R. (2014c). Estimation of the terrestrial water budget over northern China by merging multiple datasets. *Journal of Hydrology, 519*, 50–68.

Yebra, M., Dijk, A., Leuning, R., Huete, A., & Guerschman, J. (2013). Evaluation of optical remote sensing to estimate actual evapotranspiration and canopy conductance. *Remote Sensing of Environment, 129*, 250–261.

Yu, G., Wen, X., Sun, X., Tanner, B., Lee, X., & Chen, J. (2006a). Overview of ChinaFLUX and evaluation of its eddy covariance measurement. *Agricultural and Forest Meteorology, 137*, 125–137.

Yu, G., Fu, Y., Sun, X., Wen, X., & Zhang, L. (2006b). Recent progress and future direction of ChinaFLUX. *Science in China Series D, 49*(Supp. II), 1–23.

Yu, G., Zhang, L., Sun, X., Fu, Y., Wen, X., Wang, Q., Li, S., Ren, C., Song, X., Liu, Y., et al. (2008). Environmental controls over carbon exchange of three forest ecosystems in eastern China. *Global Change Biology, 14*, 2555–2571.

Yu, G., Zhu, X., Fu, Y., He, H., Wang, Q., Wen, X., Li, X., Zhang, L., Zhang, J., Yan, J., et al. (2013). Spatial patterns and climate drivers of carbon fluxes in terrestrial ecosystems of China. *Global Change Biology, 19*, 798–810.

Yuan, W., Liu, S., Yu, G., Bonnefond, J., Chen, J., Davis, K., Desai, A., Goldstein, A., Gianelle, D., Rossi, F., Suyker, A., & Verma, S. (2010). Global estimates of evapotranspiration and gross primary production based on MODIS and global meteorology data. *Remote Sensing of Environment, 114*, 1416–1431.

Yuan, W., Liu, S., Liang, S., Tian, Z., Liu, H., & Young, C. (2012). Estimations of evapotranspiration and water balance with uncertainty over the Yukon River Basin. *Water Resources Management, 26*, 2147–2157.

Yuan, W., Cai, W., Xia, J., Chen, J., Liu, S., Dong, W., Merbold, L., Law, B., Arain, A., Beringer, J., Bernhofer, C., Black, A., Blanken, P., Cescatti, A., Chen, Y., Francois, L., Gianelle, D., Janssens, I., Jung, M., Kato, T., Kiely, G., Liu, D., Marcolla, B., Montagnani, L., Raschi, A., Roupsard, O., Varlagin, A., & Wohlfahrt, G. (2014). Global comparison of light use efficiency models for simulating terrestrial vegetation gross primary production based on the LaThuile database. *Agricultural and Forest Meteorology, 192–193*, 108–120.

Zhang, K., Kimball, J., Mu, Q., Jones, L., Goetz, S., & Running, S. (2009). Satellite based analysis of northern ET trends and associated changes in the regional water balance from 1983 to 2005. *Journal of Hydrology, 379*, 92–110.

Zhang, K., Kimball, J., Nemani, R., & Running, S. (2010). A continuous satellite-derived global record of land surface evapotranspiration from 1983 to 2006. *Water Resources Research, 46*, W09522.